

# Supporting Information

## A Nanoscale Visual Exploration of the Pathogenic Effects of Bacterial Extracellular Vesicles on Host Cells

Minjae Kang<sup>1, ‡</sup>, Min Jeong Kim<sup>1, ‡</sup>, Dokyung Jeong<sup>1</sup>, Hyung-Jun Lim<sup>1</sup>, Ga-eun Go<sup>1</sup>, Uidon Jeong<sup>1</sup>, Eunyoung Moon<sup>2</sup>, Hee-Seok Kweon<sup>2</sup>, Nae-Gyu Kang<sup>3</sup>, Seung Jin Hwang<sup>3</sup>, Sung Hun Youn<sup>3</sup>, Bo Kyoung Hwang<sup>3</sup>, Doory Kim<sup>1, 4, 5, 6, \*</sup>

<sup>1</sup>Department of Chemistry, Hanyang University, Seoul 04763, Republic of Korea

<sup>2</sup>Electron Microscopy Research Center, Korea Basic Science Institute, Cheongju 28119, Republic of Korea

<sup>3</sup>R&D Center, LG H&H Co., Ltd., Seoul 07795, Republic of Korea

<sup>4</sup>Research Institute for Convergence of Basic Science, Hanyang University, Seoul 04763, Republic of Korea

<sup>5</sup>Institute of Nano Science and Technology, Hanyang University, Seoul 04763, Republic of Korea

<sup>6</sup>Research Institute for Natural Sciences, Hanyang University, Seoul 04763, Republic of Korea

‡These authors contributed equally.

\*Corresponding author: doorykim@hanyang.ac.kr

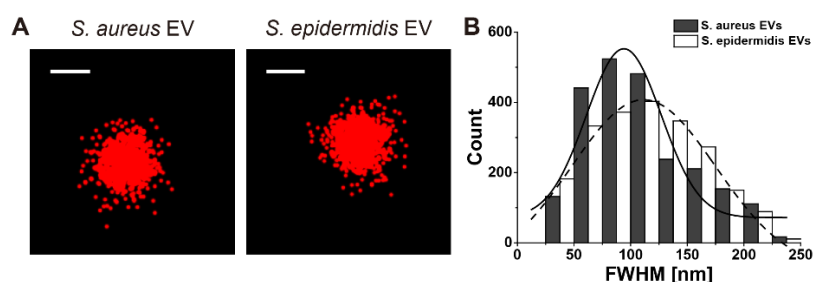


**Fig. S1** Representative STORM images of EVs purified from *S. aureus* and *S. epidermidis*. (A) Representative STORM images of purified *S. aureus* (left) and *S. epidermidis* (right) EVs labeled with Nile red. Scale bar: 100 nm. (B) Size distribution of EVs measured from the STORM images of Nile red-stained purified EV samples. The full width at half maximum (FWHM) of a single-molecule distribution was used as the diameter of each EV particle.

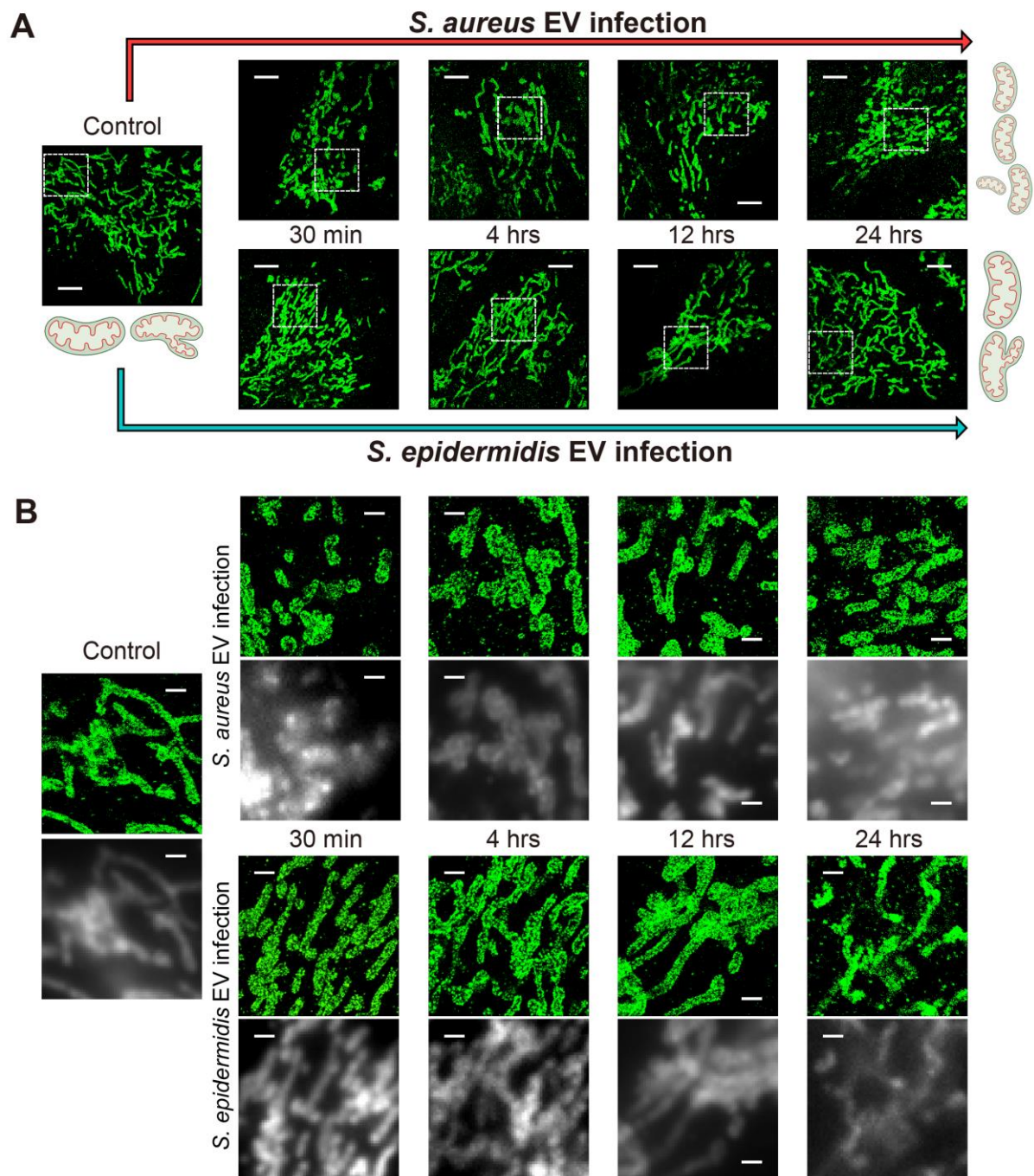


**Fig. S2** Mitochondrial change during EV-mediated infection. **(A)** Representative STORM images of mitochondria in epithelial keratinocyte (HaCaT) cells treated with *S. aureus* EVs (top) or *S. epidermidis* EVs (bottom) at different times. Schematic diagrams are shown together. **(B)** Enlargement of the boxed region in **(A)** to compare the diffraction-limited images (bottom) and STORM images (top). Scale bars: 5  $\mu\text{m}$  (top), 1  $\mu\text{m}$  (bottom).

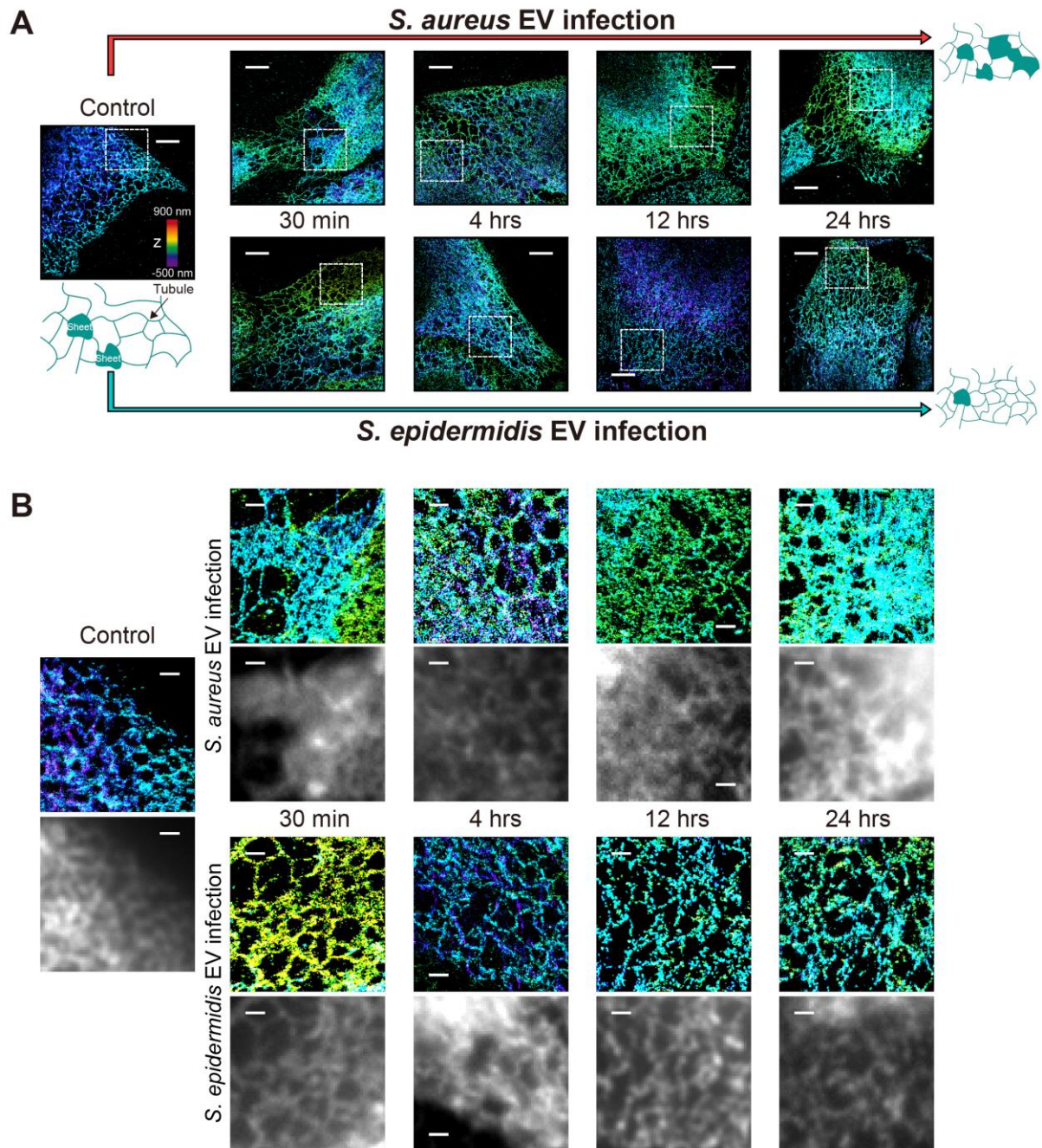


**Fig. S3** Transformation of endoplasmic reticulum (ER) between sheet and tubular structures by EV infection. **(A)** Representative STORM images of ER in epithelial keratinocyte (HaCaT) cells treated with *S. aureus* EVs (top) or *S. epidermidis* EVs (bottom) at different times. Schematic diagrams are shown together. **(B)** Enlargement of the boxed region in **(A)** to compare the diffraction-limited images (bottom) and STORM images (top). Scale bars: 5  $\mu\text{m}$  (top), 1  $\mu\text{m}$  (bottom).



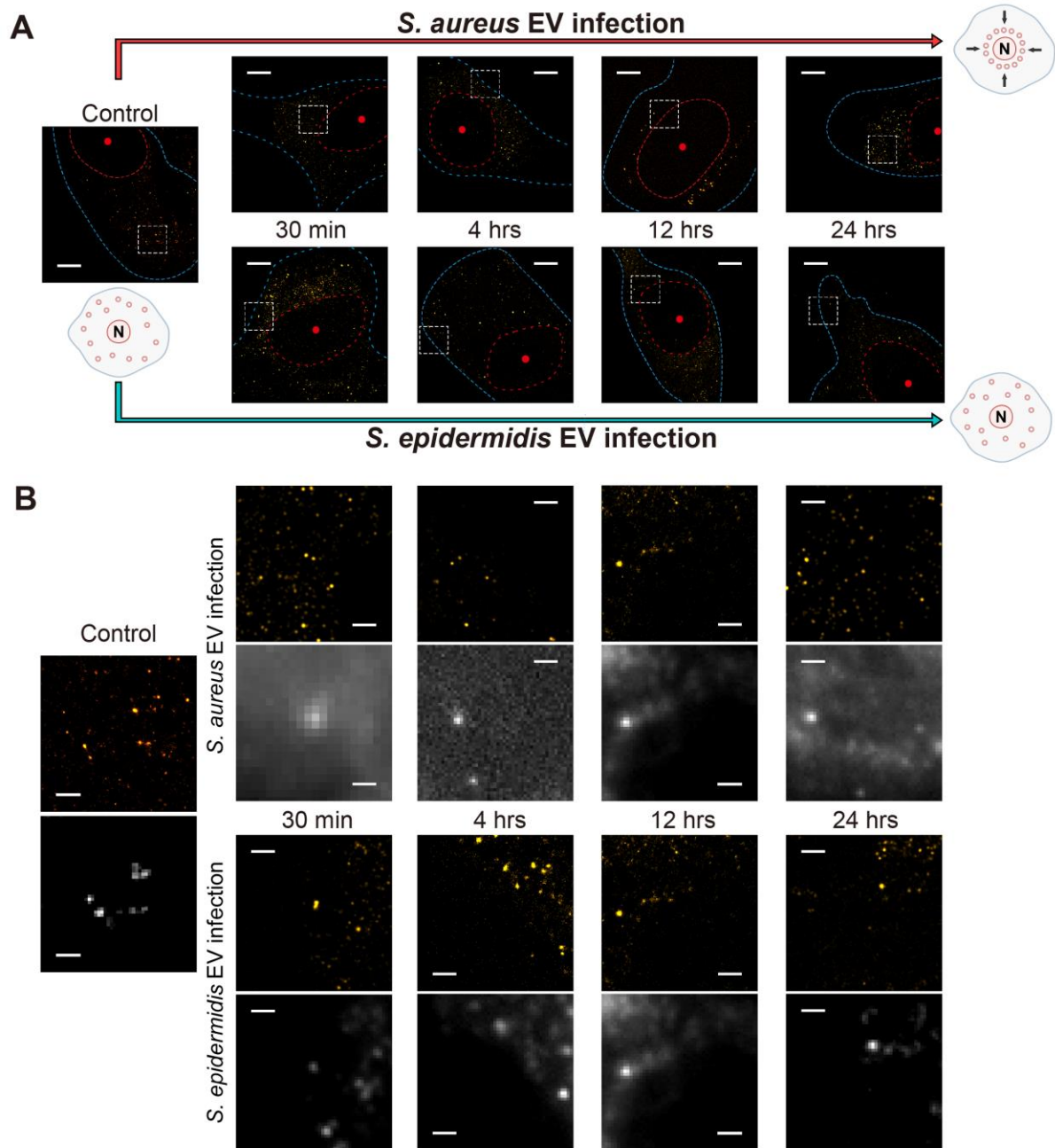


**Fig. S4** Lysosome distribution change during EV-mediated infection. **(A)** Representative STORM images of lysosomes in epithelial keratinocyte (HaCaT) cells treated with *S. aureus* EVs (top) or *S. epidermidis* EVs (bottom) at different times. Schematic diagrams are shown together. Dashed lines: cell membrane boundary (blue) and nucleus boundary (red). **(B)** Enlargement of the boxed region in **(A)** to compare the diffraction-limited images (bottom) and STORM images (top). Scale bars: 5  $\mu\text{m}$  (top), 1  $\mu\text{m}$  (bottom).

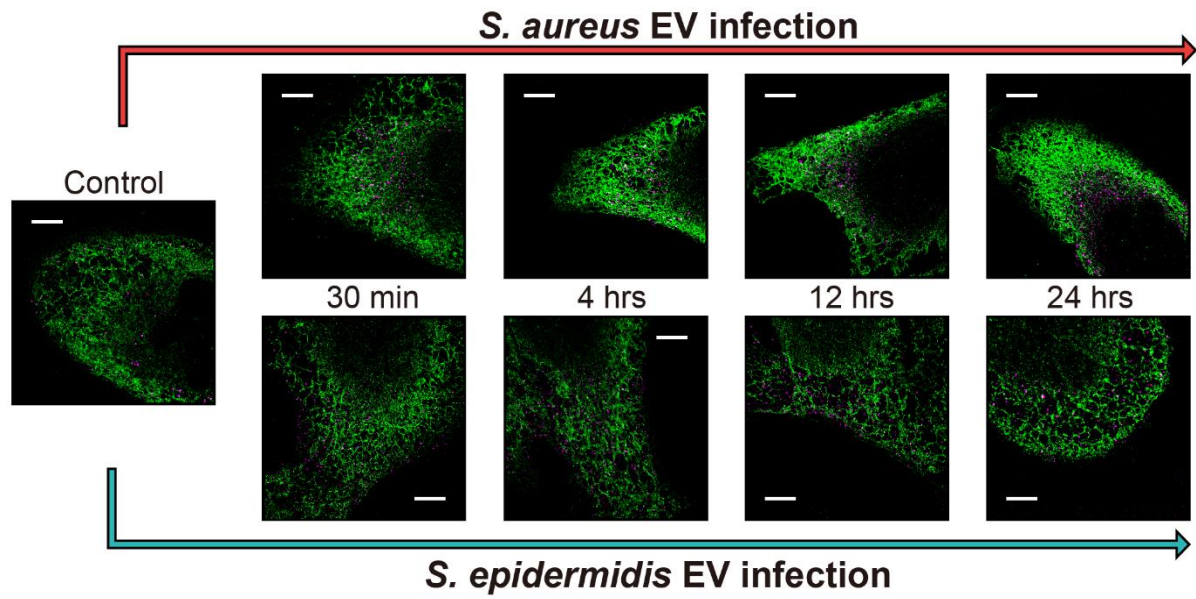


**Fig. S5** Representative two-color STORM images of ER (green) and lysosomes (magenta) in epithelial keratinocyte (HaCaT) cells treated with *S. aureus* EVs (top) or *S. epidermidis* EVs (bottom) at different times. Scale bar: 5  $\mu\text{m}$ .

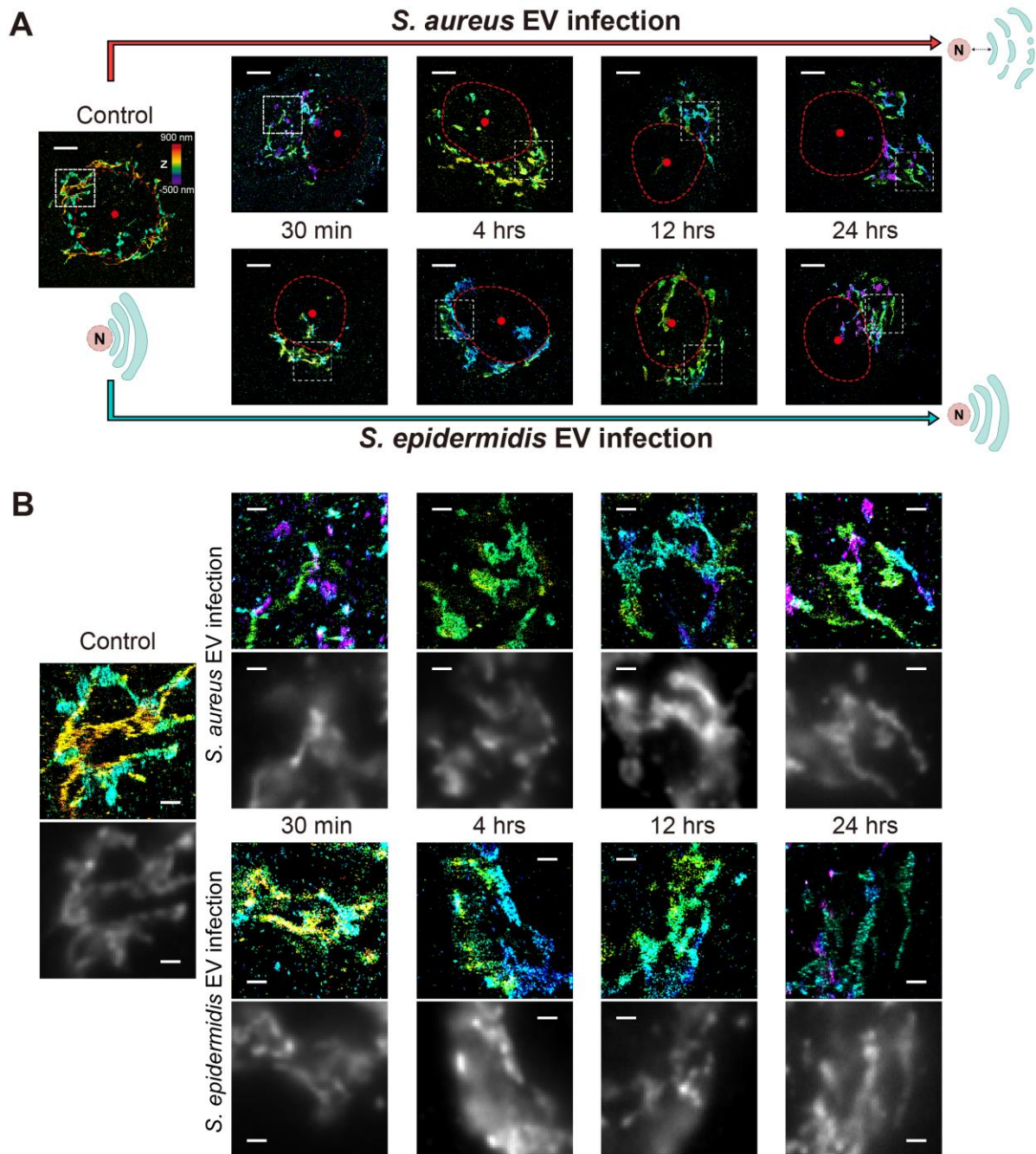


**Fig. S6** Golgi dispersion and fragmentation by *S. aureus* EV infection. (A) Representative STORM images of Golgi in epithelial keratinocyte (HaCaT) cells treated with *S. aureus* EVs (top) or *S. epidermidis* EVs (bottom) at different times. Schematic diagrams are shown together. (B) Enlargement of the boxed region in (A) to compare the diffraction-limited images (bottom) and STORM images (top). Scale bars: 5  $\mu\text{m}$  (top), 1  $\mu\text{m}$  (bottom).



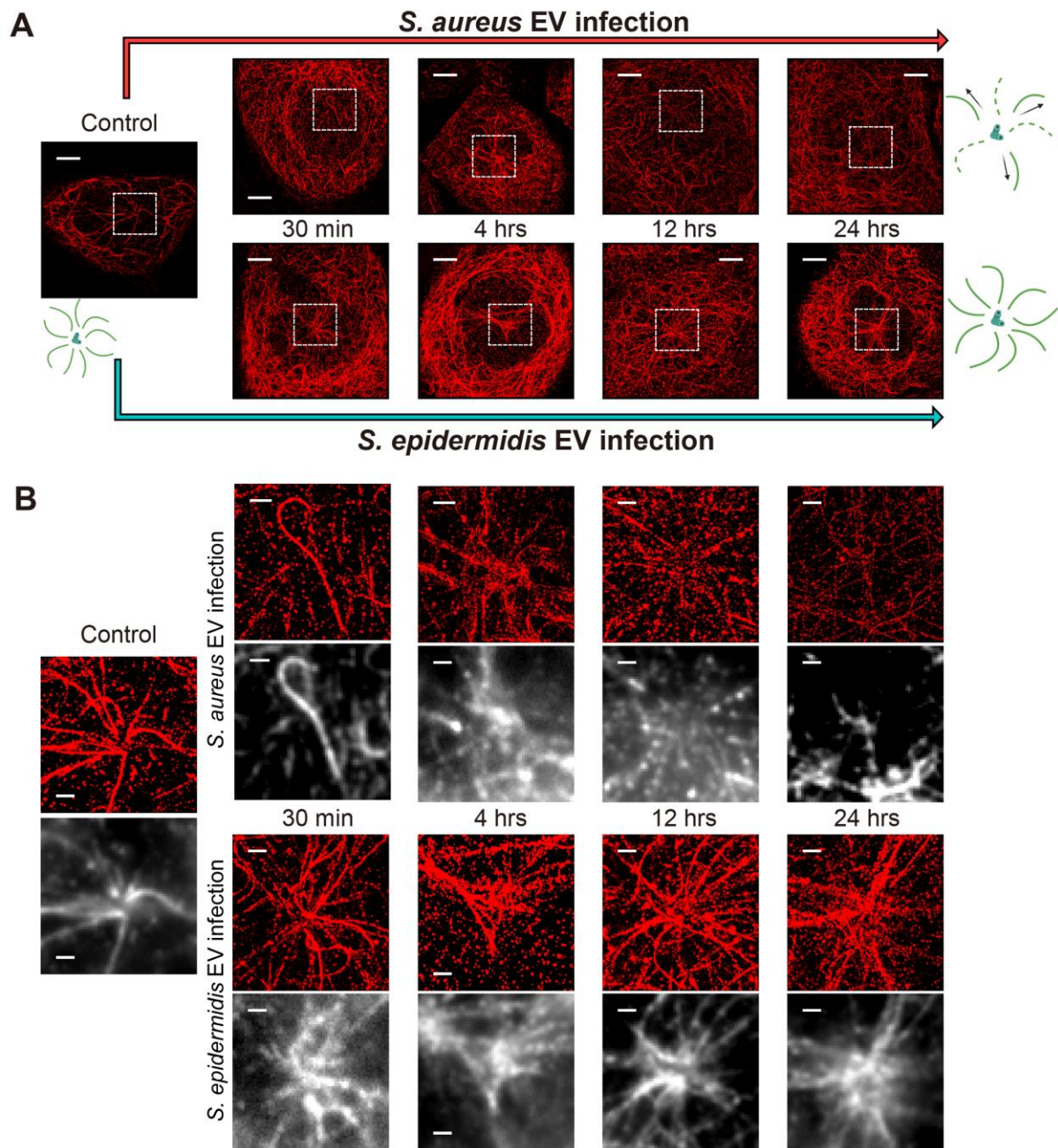


**Fig. S7** Depolymerized microtubule organizing center (MTOC) by *S. aureus* EV infection. **(A)** Representative STORM images of acetylated tubulin to reveal the MTOC in epithelial keratinocyte (HaCaT) cells treated with *S. aureus* EVs (top) or *S. epidermidis* EVs (bottom) at different times. Schematic diagrams are shown together. **(B)** Enlargement of the boxed region in **(A)** to compare the diffraction-limited images (bottom) and STORM images (top). Scale bars: 5  $\mu\text{m}$  (top), 1  $\mu\text{m}$  (bottom).

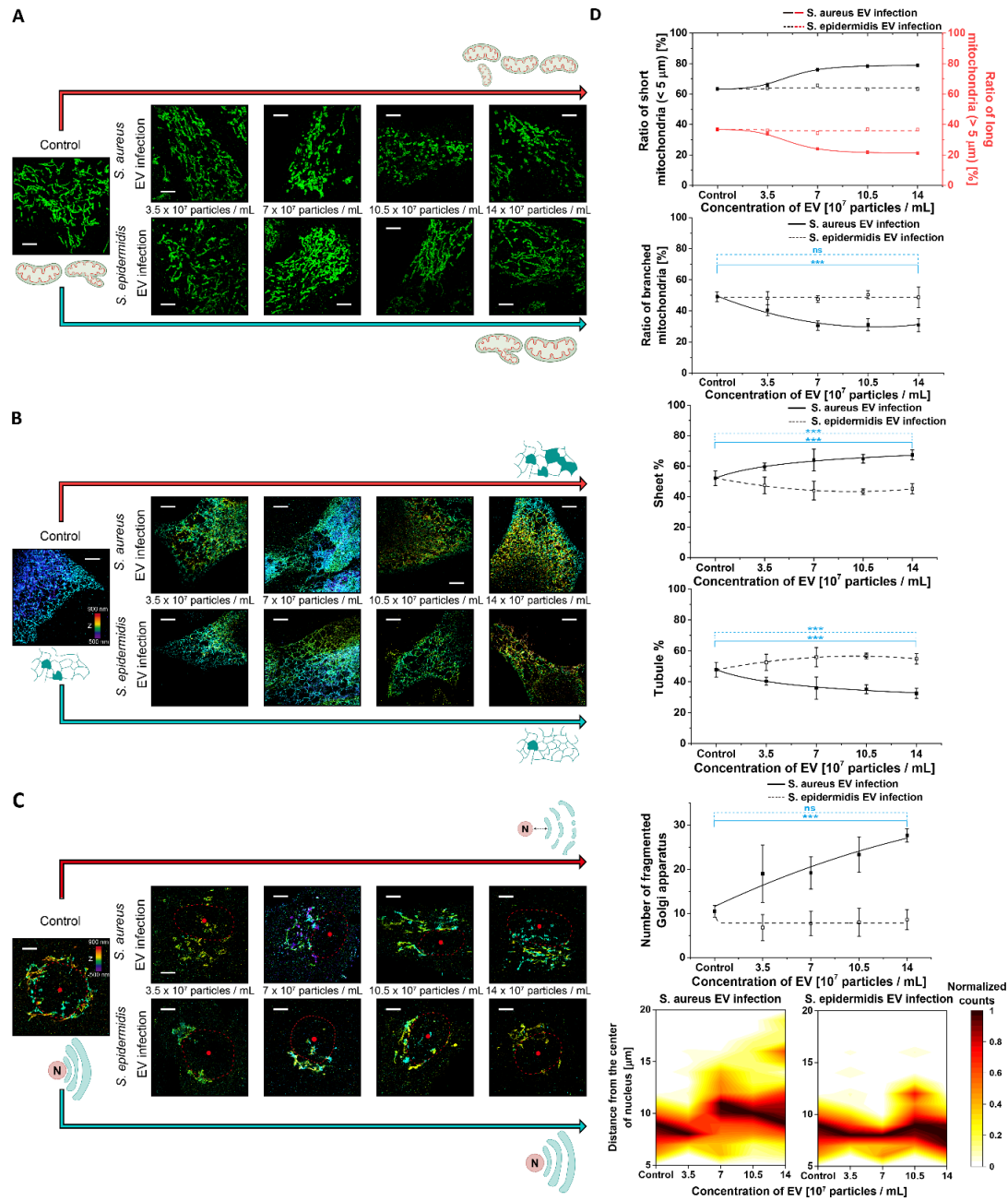


**Fig. S8** Representative STORM images of (A) mitochondria, (B) ER, and (C) Golgi in epithelial keratinocyte (HaCaT) cells treated with *S. aureus* EVs (top) or *S. epidermidis* EVs (bottom) at different concentration of EVs after 30 min of EV infection. (D) Quantitative analysis of the ultrastructural changes of mitochondria in terms of the ratio of long (with > 5 μm longest diameter) and short mitochondria (with < 5 μm longest diameter) and ratio of branched mitochondria from STORM images (n = 10, mean±SD), ER in terms of the percentage of sheet-like and tubular structures (n = 10, mean±SD), Golgi apparatus in terms of the number of Golgi fragments and the radial distribution from the center of the nucleus. (n = 10, mean±SD) (ns: p > 0.05, \*\*\*p < 0.001) Scale bars: 5 μm



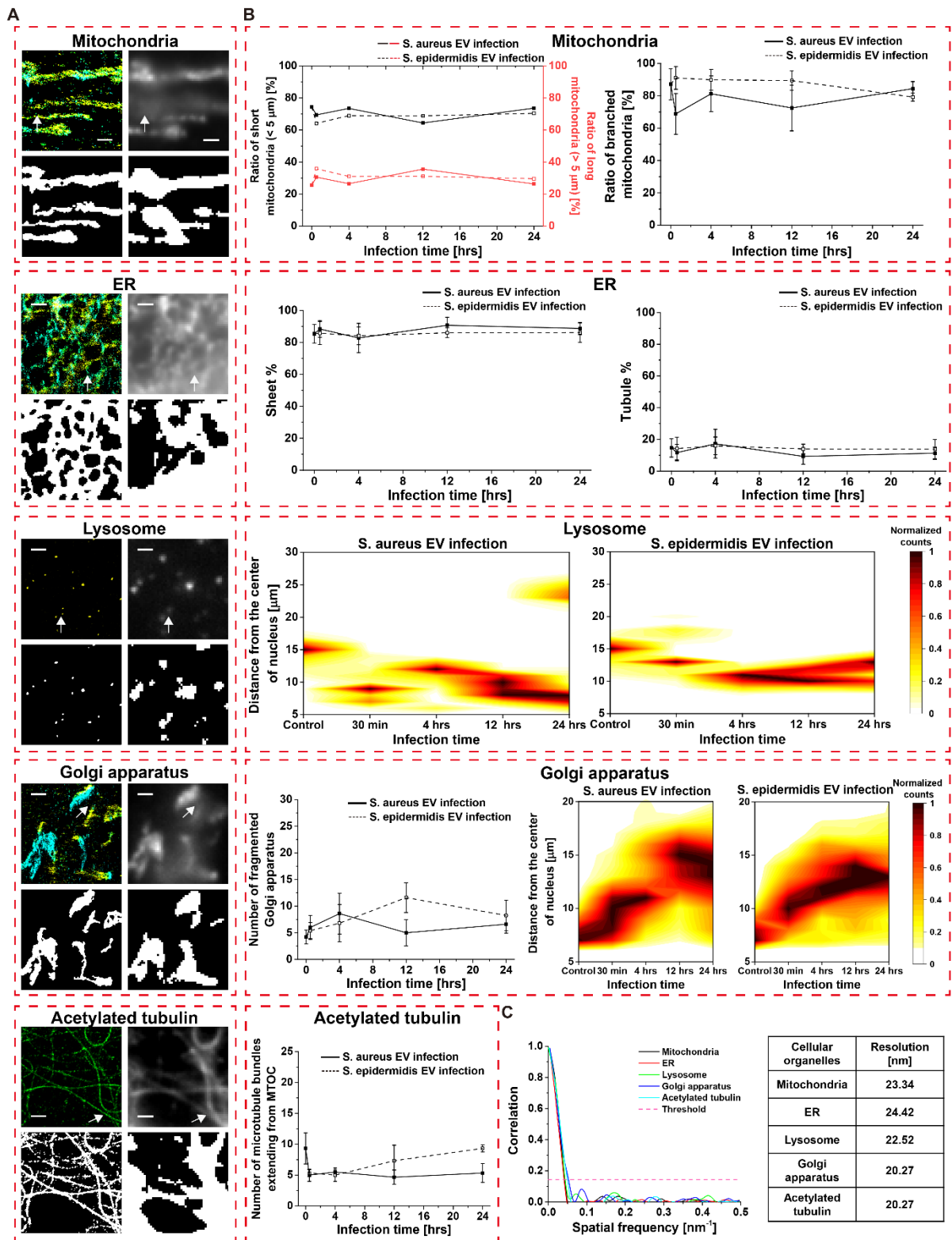


**Fig. S9** Super-resolution imaging capability of STORM in this study. (A) Ultrastructures of various organelles revealed by STORM imaging compared with diffraction-limited fluorescence microscopy. The bottom row shows the identified boundaries of each organelle segment, indicating errors in detecting the fine structures of the

organelles due to optical blurring. Arrows: filtered background signal. Scale bar: 1  $\mu\text{m}$ . (B) Quantitative analysis of the structural changes of organelles from the diffraction-limited fluorescence images corresponding to the STORM images analyzed in Figs. 1, 3, and 4. (C) Fourier ring correlation (FRC) analysis of STORM images for each organelle.

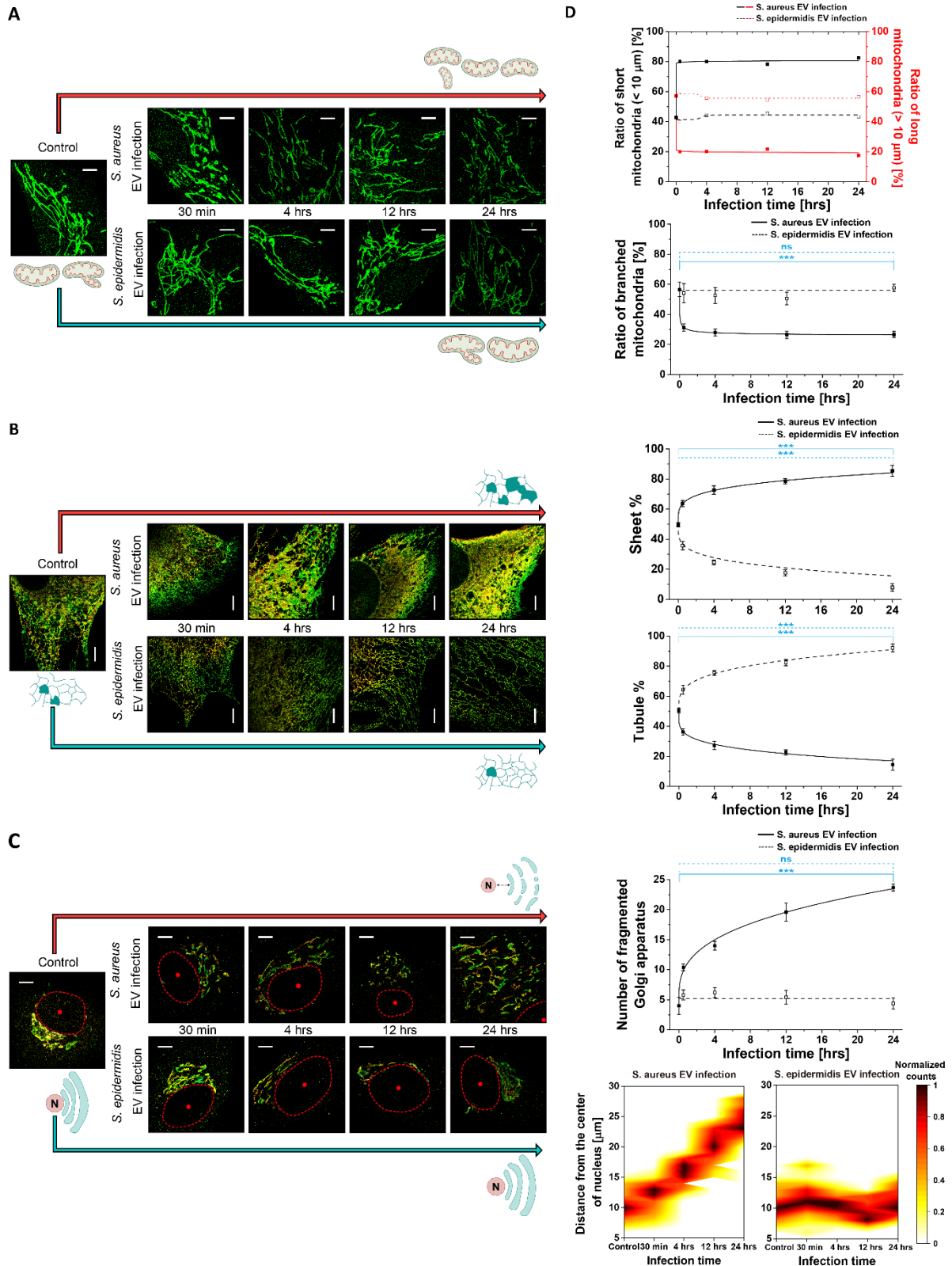


**Fig. S10** Representative STORM images of (A) mitochondria, (B) ER, and (C) Golgi apparatus in human dermal fibroblasts (HDF) cells treated with *S. aureus* EVs (top) or *S. epidermidis* EVs (bottom) at different times. (D) Quantitative analysis of the STORM images of each organelle. (the ratio of long (with > 10  $\mu\text{m}$  longest diameter)



and short mitochondria (with < 10 µm longest diameter) and the ratio of branched mitochondria; percentage of ER tubular and sheet-like structures; the number of Golgi fragments and radial distribution from the center of the nucleus). (n= 10, mean±SD) (ns: p > 0.05, \*\*\*p < 0.001) Scale bar: 5 µm.

**Supplementary Movie 1.** The 3D reconstructed HVEM movie of a representative mitochondrion in epithelial keratinocyte (HaCaT) cells as a control sample.

**Supplementary Movie 2.** 3D reconstructed HVEM movie of a representative mitochondrion in epithelial keratinocyte (HaCaT) cells treated with *S. aureus* EVs.

**Supplementary Movie 3.** 3D reconstructed HVEM movie of a representative mitochondrion in epithelial keratinocyte (HaCaT) cells treated with *S. epidermidis* EVs.

**Supplementary Movie 4.** The 3D reconstructed HVEM movie of a representative Golgi in epithelial keratinocyte (HaCaT) cells as a control.

**Supplementary Movie 5.** 3D reconstructed HVEM movie of a representative Golgi in epithelial keratinocyte (HaCaT) cells treated with *S. aureus* EVs.

**Supplementary Movie 6.** 3D reconstructed HVEM movie of a representative Golgi in epithelial keratinocyte (HaCaT) cells treated with *S. epidermidis* EVs.